

OPEN TYPE QUAY STRUCTURES UNDER PROPELLER JETS

Yalcin Yuksel¹, Selahattin Kayhan¹, Yesim Celikoglu¹ and Kubilay Cihan¹

In recent years, dramatically increases in ship dimensions and installed engine power, introduction of new type of special purpose ships and use of roll-on/roll-off, ferries, container ships can cause damage which in many cases threatens to undermine berth structures. Vessel jets of these types of ships can change flow area and cause erosion and scour around foundation of berth structures. Due to the damages in berth structures maintenance and repair cost may increase and also cause management losses. For this reason vessel jet induced the flow area around the berth structures during ships berthing and un-berthing operations are extremely important factor for the port structure design.

This study is related with investigation of the flow characteristics at the sea bed around the pile, experimentally. Vessel jets were simulated both as circular wall jet and also propeller jet. The objective of this study is to determine the sea bed shear stress and velocity profiles along the jet axis for open type wharf structures (around a cylindrical piles and also on the slopes). Hot film anemometers were used to measure the magnitude of the bed shear stresses. The results from propeller jet experiments explained the erosion over the slopes. Bed shear and velocity profile measurements were carried out on the rigid bed conditions.

Keywords: quay structures; propeller jets; erosion

INTRODUCTION

The problem of propeller jet induced erosion has significantly risen during the last three decades due to the increase of maneuverability of the ships. Therefore, the propeller induced scour need to be considered in the design of the quay structures.

There are two main types of trust systems (Fig.1):

- Propellers (conventional propeller, azimuthal system and bow thruster).
- Water (hydro) jets.

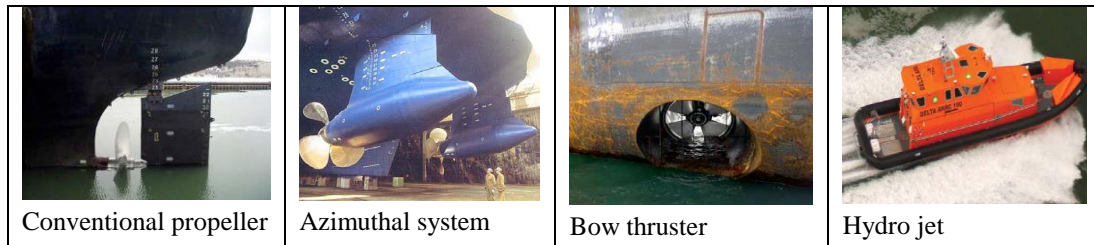


Figure 1 Ship thrust systems.

Erosion caused by strong flows generated by vessel propulsion systems have become significant importance to protect the bed around the piles and in the design of armoured slopes under open piled quay structures. For example, velocities at propeller jets at the exits of propellers can be 11 to 12 m/s with resulting bed velocities from 3 to 4 m/s. Depending on circumstances, the average depth of scour could reach as much as 0.5m per month and may be more.

The investigations of predicting the velocity within the ship's propeller jet, which can lead to seabed scouring, are of particular interest for the design of marine structure. Sumer and Fredsøe (2002) and Whitehouse (1998) described seabed scouring mechanism around the coastal structures in detail.

A rotating ship propeller generates a turbulent continuous stream of fast moving water flow known as the propeller-induced jet (Fig. 2).

Propeller induced scour problems have been investigated experimentally using physical models such as Blaauw and Van de Kaa (1978), Bergh and Cederwall (1981), Verhey (1983), Veldhoven (2001), Schokking (2003) and Lam et al. (2011).

The velocity distribution of free-propeller jet is assumed to have the shape of a normally distributed profile (Fig. 3). The velocity profile of a submerged water jet from an orifice varies also according to Gaussian normal probability function at each cross section (Fig. 4). Water jet is categorized into a zone of flow establishment and a zone of established flow. In the zone of flow establishment the maximum

¹ Civil Engineering Department, Yildiz Technical University, Davutpasa Campus, Esenler, Istanbul, Turkey

velocity is constant while the lateral distribution is expanding. The region with constant maximum velocity has a pronounced potential core. The lateral section of potential core is contracting due to the turbulent mixing between the core and the surrounding fluid. In the zone of established flow, the maximum velocity starts to decay along the rotation axis. In this zone, entrainment of the surrounding fluid is balanced by reduction in the jet velocity. In addition, the water jet was axisymmetrical with the entire jet being mirrored about the central axis (Lam et al., 2011).

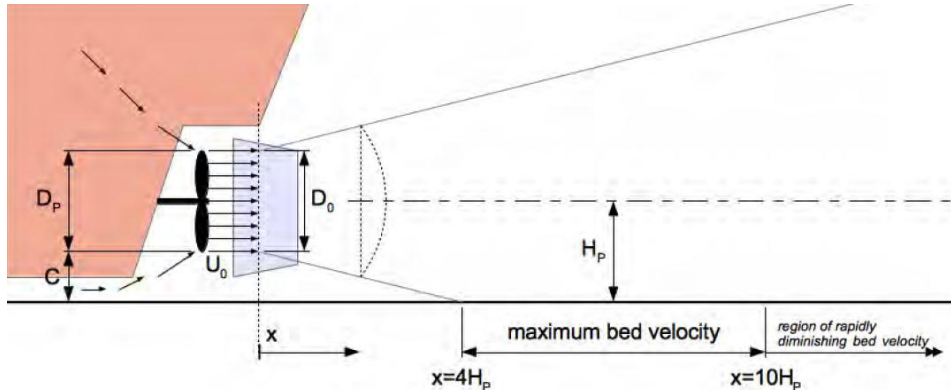


Figure 2 Simplified diagram of propeller-induced jet (Billiton, 2010).

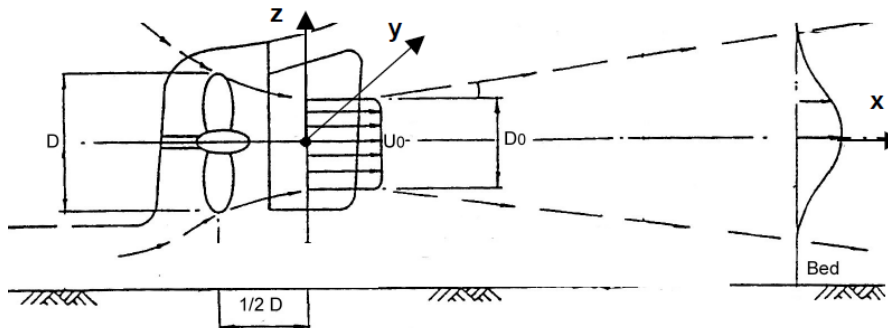


Figure 3 Velocity distribution at exit from the propeller and in developed flow (Schokking, 2003).

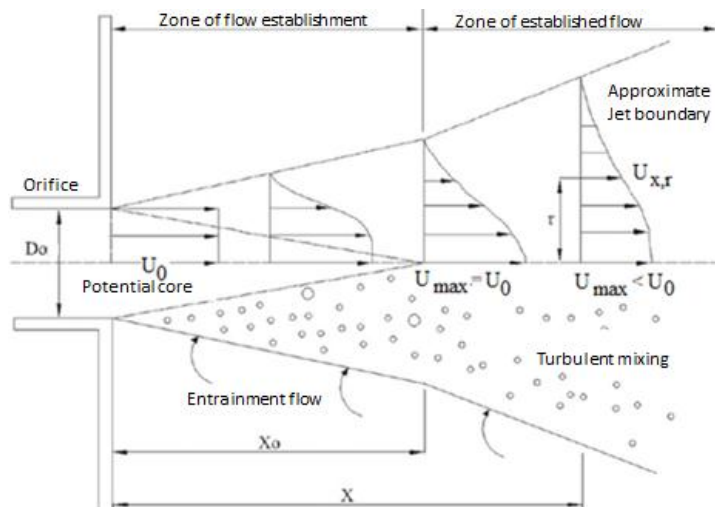


Figure 4 Schematized representation of a diffusing jet from an orifice (Lam et al., 2011).

The erosion protection of the slope under an open piled berth structure depends upon the angle of the slope, the coarseness of the materials in front of the filling, the danger of erosion from wave action at the upper part of the filling, the danger of erosion from propeller current from the main ship propellers and the ship bow and stern thrusters at the lower part of the filling (PIANC, 1997). Despite

all of the studies on this problem, few literatures could be found on the effect of different slopes for the scouring process at berthing structures.

In recent years, numerical and experimental studies were carried out for the hydrodynamics of both water jet and propeller jet. Yuksel and Yuksel (2010) investigated 3D submerged jet flow around a pile. They used ADV to obtain the jet velocity distributions. They predicted the flow field around pile with realizable k- ϵ turbulence.

Cihan et al. (2012) also carried out an experimental investigation for the eroded area on armoured slopes under berth structures for movable bed conditions. They considered three different cases which were armoured layer with and without protection layer and pile on armoured layer with protection layer. Velocity and scour measurements were conducted in their experiments and armour layer damages on the slope were defined using a damage level parameter. Experiments show that damage parameter has a good relation with the densimetric Froude number and slope angles. The volume of eroded and accumulated area increases with increasing rpm values for all cases and slope angles.

Densimetric Froude number was defined as,

$$Fr_d = \frac{U_0}{\sqrt{gd_{50}((\rho_s - \rho)/\rho)}} \quad (1)$$

where U_0 jet exit velocity, d_{50} median sediment diameter, ρ_s sediment density and ρ water density. Five different Froude Numbers were considered between 3.6 and 6.2 in the experiments. Froude Numbers were calculated with median coarse gravel diameter (d_{50}). The damage level was defined by

$$S = \frac{-A}{D_{n50}^2} \quad (2)$$

where S is the damage level, $-A$ is the erosion area around the still water level and D_{n50} is the nominal diameter for rock. The start of the damage was defined by critical densimetric Froude Numbers ($Fr_{d,cr}$) which were given in Table 1 for all cases.

Slope (m)	2.5	2.0	1.5
$Fr_{d,cr}$	3.72	3.68	3.28

Schokking (2003) worked on bow thruster-induced damage over the slopes (Fig. 5). He measured the velocity profiles and defined the turbulence structures. Damage location was investigated. He concluded that the free-propeller jet had a similar diverging pattern as the ducted-propeller jet. The velocity decrease with distance from the propeller was higher for the free-propeller jet than the ducted-propeller jet. The most severe damage was occurred on the toe of the slope.

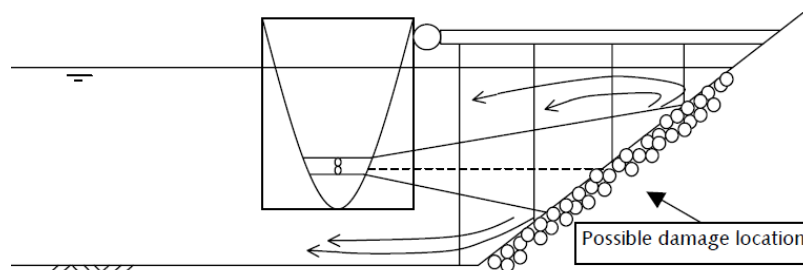


Figure 5 Side view of the propeller jet on the slope (Schokking, 2003)

In order to provide a sufficient protection against scouring caused by propeller jet, it is necessary to obtain the effect on armoured slope angle on the jet mechanism.

The objective of this study is to determine the influence of the vessel jet, which can lead to seabed scouring for the pile type marine structures. Two type of vessel jet were considered during the experiments which were free water wall jet and propeller jet without hub. These jets were simulated by conventional propeller and hydro jet. The bed shear stresses were measured along the jet axis in front and back of the piles with jet flow.

EXPERIMENTAL STUDY

This study had two steps; water jet and free propeller jet experiments. Experiments were performed in two different laboratory flumes in Hydraulic and Coastal Engineering Laboratory, Yıldız Technical University.

i) Experimental Setup With Water Jet

The experiments were conducted in a laboratory tank (length 3 m, width 0.62 m and height 1 m) by installing a cylindrical pile on horizontal and rigid bottom (Figure 6). The location of the pile and the water jet were kept constant but discharges were different. Velocity and shear stresses were measured around the pile and along the jet axis on upstream and downstream of the pile with respect to the jet exit diameter of the times distances. The water depth was kept constant 38 cm in the channel. The nozzle diameter was $D_0=22$ mm and the pile diameter was $d_0=48$ mm. Velocity measurements were performed with Acoustic Doppler Velocimeter (ADV) and bed shear stress measurements were achieved with Hot Film Anemometer. Experiments were carried out with three different jet flow Reynolds numbers as 38280, 43340 and 48180. Reynolds number was defined as,

$$Re = \frac{U_0 D_0}{\nu} \quad (3)$$

where U_0 water jet velocity at the exit of the pipe, D_0 nozzle diameter and ν kinematic viscosity of water.

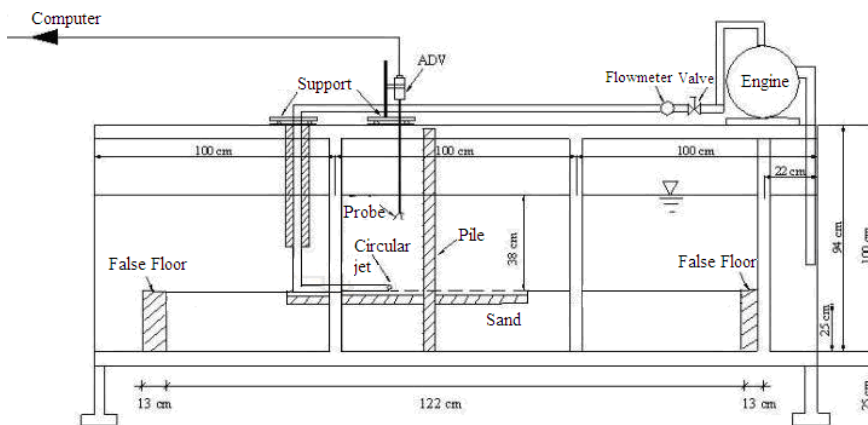


Figure 6 Cross-section of the water tank

A pump supplied the water jet and the flow rate was controlled by a gate-valve. Discharge was measured by an electronic flow meter. The experiments were carried out on the rigid bottom.

ii) Experimental Setup For Free-Propeller Jet

The second water tank was 12m long, 1.0m wide and 1m high. Both sides of flume were made of glass and it had a propeller system inside. Propeller rotation was controlled with an automation panel. The experimental set-up was presented in Figure 7. The propeller was located at 19 cm above the bed to demonstrate the free-propeller above the bed. In the experiments three different slope angles (1/1.5, 1/2, 1/2.5) were defined. The fixed water depth was 48 cm above the bed which corresponds to the top of the slope. The propeller diameter was 70 mm and its number of blades was four. The pile diameter was 40mm. Bed shear stresses over the rigid smooth slopes were measured with hot film anemometers.

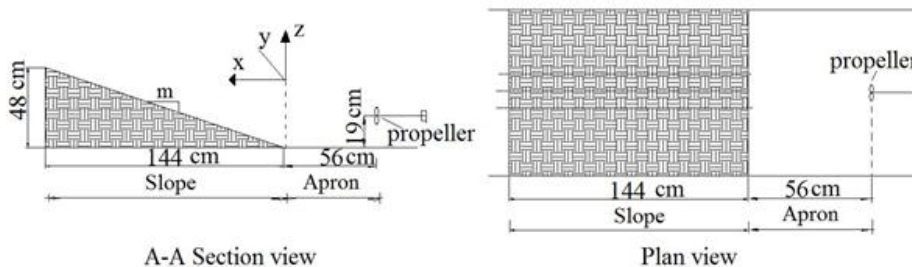


Figure 7 Experimental set up for free-propeller jet

Three different flow Reynolds numbers were considered as 43290, 48315 and 53340 in the experiments. Flow Reynolds number was defined by

$$Re = \frac{U_0 D_p}{\nu} \quad (4)$$

where the efflux velocity (U_0) is the maximum velocity at the face of the propeller (Fuehrer and Römisch, 1977), which is

$$U_0 = 1.59 n D_p \sqrt{C_t} \quad (5)$$

where n is the rotational speed of the propeller in revolution per second, D_p is the propeller diameter in meters and C_t is the thrust coefficient of the propeller, ν kinematic viscosity of water. The thrust coefficient (C_t) was 0.35 and the blade area ratio (β) was 0.5 for the propeller which were used in the experiments. The rotational speeds were 560 rpm, 630 rpm and 695 rpm.

RESULTS and DISCUSSION

i) Water Jet Case

The hydrodynamic conditions were explained around the piles under wall jet effects. Velocity measurements were performed along the jet axis in several sections at the upstream and downstream of the pile. The measurement scheme was given in Figure 8. x defined with horizontal distance from the nozzle to downstream sections.

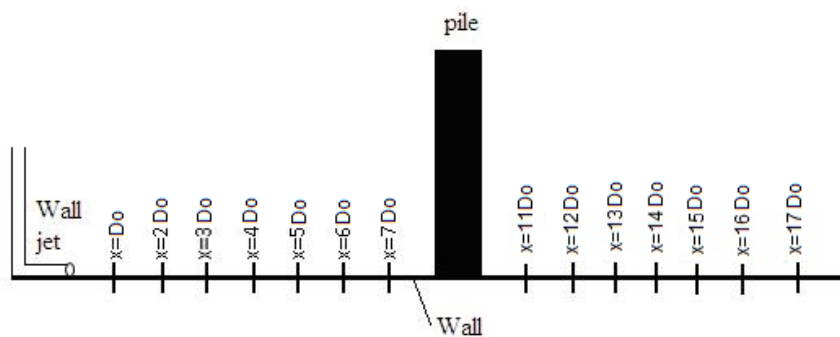


Figure 8 Wall jet velocity and shear stress measurements scheme (along the jet axis)

Figure 9 shows non dimensional horizontal velocity component (u) profiles in x direction along the jet axis at the upstream side of the pile for $Re=43340$. It is shown that the velocity profiles decay with the distance from jet in Figure 9. The same trend is observed for the other flow Reynolds numbers. Maximum velocities occurred at $x=D_0$ for all Reynolds numbers. Maximum velocity is $1.08U_0$ and at $z=1.14D_0$ for $Re=43340$. The values for the other Reynolds numbers are given in Table 2.

Table 2 Maximum velocities and their locations along the wall at the upstream side of the pile for all flow Reynolds numbers			
Re	Maximum velocities (u_m)	Horizontal distance from the jet exit (x)	Vertical distance from the wall (z)
38280	$1.09U_0$	D_0	$1.05D_0$
43340	$1.08U_0$	D_0	$1.14D_0$
48180	$1.07U_0$	D_0	$1.14D_0$

Figure 10 shows non dimensional horizontal velocity component (u) variations along the jet axis at the downstream side of the pile for $Re=43340$. It is seen that velocity variations are small at downstream of pile. However velocities changes from $-0.21U_0$ to $0.046U_0$ at $x=11D_0$. This is because the decreasing of the jet effect and the reverse flow due to the pile. This effect is seen at most $x = 11D_0$. It is observed that velocities decreased with the distance from the pile. The same trend is observed for other Reynolds numbers. Negative velocities occur at $x=11D_0$ for all Reynolds numbers. Maximum velocity occur at $x=16D_0$. Maximum velocity is $0.13U_0$ and at $z=1.27D_0$ for $Re=43340$. Maximum

negative velocity occur at $x=11D_0$. Its value is $-0.21U_0$ at $z=2.18D_0$. The values for other Reynolds numbers are given in Table 3. When the velocity profiles are examined, it is seen that the water jet flow behaves like a wall jet.

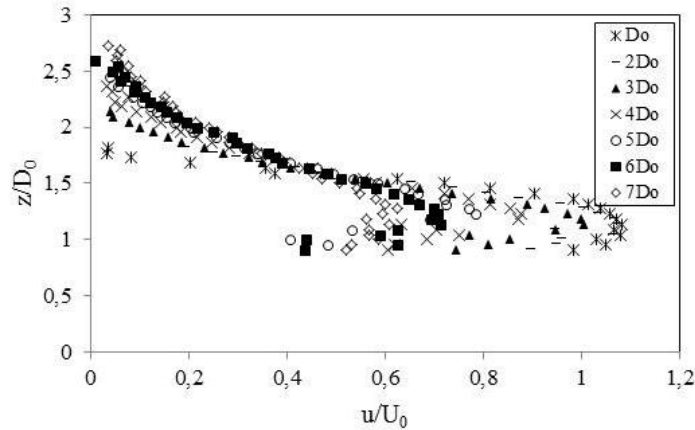


Figure 9 Non dimensional velocity component in x direction along the jet axis at the upstream side of the pile for $Re=43340$.

Table 3 Maximum velocity component and their locations along the jet axis at the downstream side of the pile for all flow Reynolds numbers			
Reynolds Numbers	Maximum velocities (u_m)	Horizontal distance from the pile (x)	Vertical distance from the wall (z)
38280	$0.114U_0$	$4D_0$	$1.23D_0$
43340	$0.13U_0$	$6D_0$	$1.27D_0$
48180	$0.11U_0$	$4D_0$	$0.91D_0$

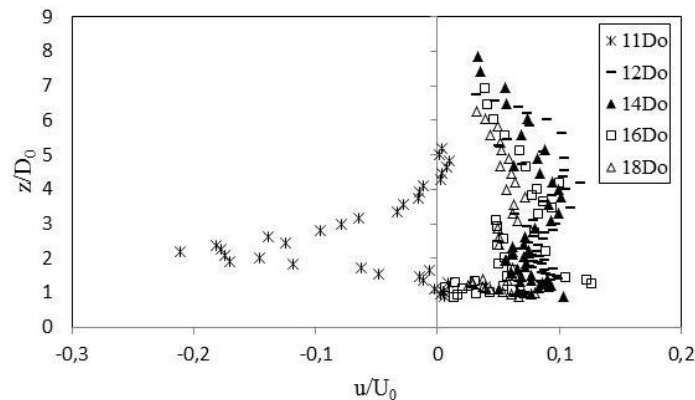


Figure 10 Non dimensional velocity component in x direction along the jet axis at the downstream side of the pile for $Re=43340$.

Bed shear stress measurements were performed along the jet axis in several sections at the upstream and the downstream of the pile. The measurement scheme was given in Figure 8. Again x defined with horizontal distance from the jet exit in upstream and downstream sections.

Non-dimensional shear stresses measurements at the upstream and the downstream of the pile respect to the shear stress at jet exit ($x = D_0$) were obtained. As bed shear stresses increase towards the pile at the upstream of the pile along the jet axis, they decrease away from the pile by increasing Reynolds number (Figure 11). The maximum magnitude of the bed shear stress was found in front of the pile where the shear stress 3.5 times compared to jet exit for $Re=43340$.

Bed shear stress measurements were also carried out around of the pile. Around of the pile bed shear stress measurements were performed at different angles ($\theta=0^\circ, 15^\circ, 30^\circ, 45^\circ, 60^\circ, 75^\circ, 90^\circ, 105^\circ, 120^\circ, 135^\circ, 150^\circ, 165^\circ$ and 180°). The measurement scheme is given in Figure 12.

In figure 13, the magnitude of the bed shear stresses increase from $\theta=0^\circ$ to $\theta=75^\circ$ at the upstream of the pile. The magnitude of the bed shear stresses decrease after $\theta=75^\circ$ at the downstream of the pile.

The maximum bed shear stress is observed at $\theta=75^\circ$ where 2.4 times of the shear stress at the nozzle (jet exit) for $Re=43340$. The magnitude of the bed shear stresses also increase with increasing Reynolds number.

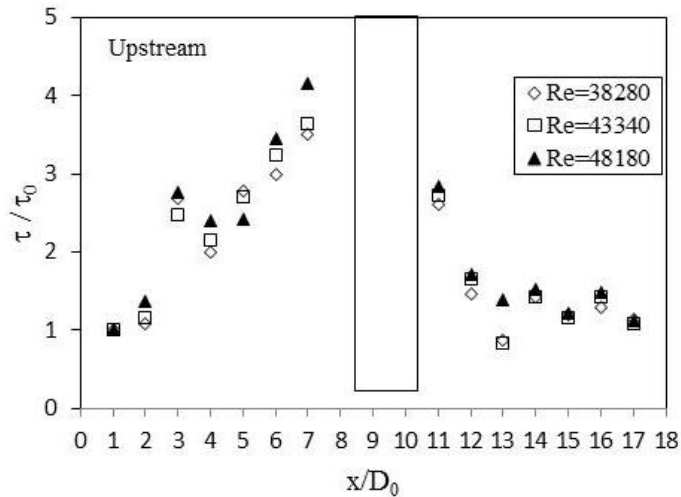


Figure 11 Non dimensional bed shear stresses measurements at the upstream and the downstream of the pile along the jet axis.

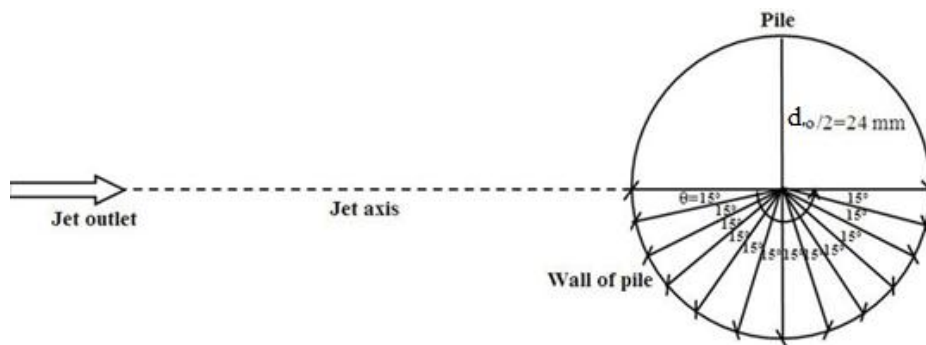


Figure 12 Wall jet bed shear stress measurement scheme around of the pile.

ii) Free-Propeller Jet Case

In order to explain the hydrodynamic conditions of the propeller, an open type wharf was designed with a pile with the slopes, the pile placed at the toe of the slopes as shown in Fig. 14. Velocity and bed shear stress measurements were done along the jet axis in several sections at the upstream and the downstream of the pile. x is the horizontal distance from the propeller model to the downstream section.

Figure 15 shows that the velocity profiles along the propeller jet axis were measured (Cihan et al., 2012). The measurement presented the velocity profiles for different slope angles in order to see the effect of the slopes. The measurements were taken for 690 rpm. The velocity distributions are almost the same for different slope angles, which means that there is no slope angle effect on the velocity profiles. In the first part of the influence of the propeller jet was clearly visible, causing the indentation in the velocity profile. This velocity profile slowly disappeared. This influence of the propeller jet was obviously seen close to the propeller ($2 \leq x/D_p$) and this influence disappeared after $x/D_p \geq 3$. The

maximum axial velocities situated almost at the same points which are $z/D_p = \pm 0.3$. This results have a good agreement with Schokking (2003)'s results.

Figure 16 shows the measured velocity profiles behind the pile. At $7d_0$ just behind the pile, the negative velocities were observed near bottom. Reverse flows are observed more clearly for the steepest slope ($m=1.5$). The velocities decrease with increasing the slope. The velocity profiles become uniform behind the pile and decay away from the pile.

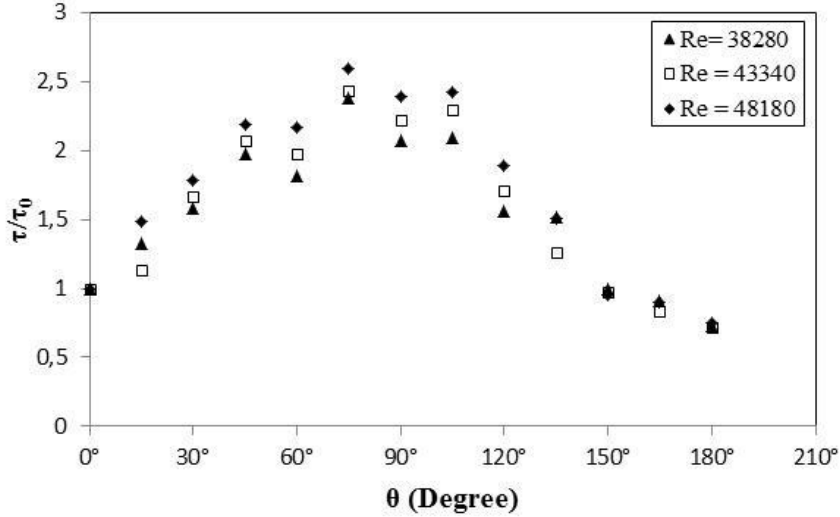


Figure 13 Non dimensional bed shear stresses around of the pile for $Re=43340$.

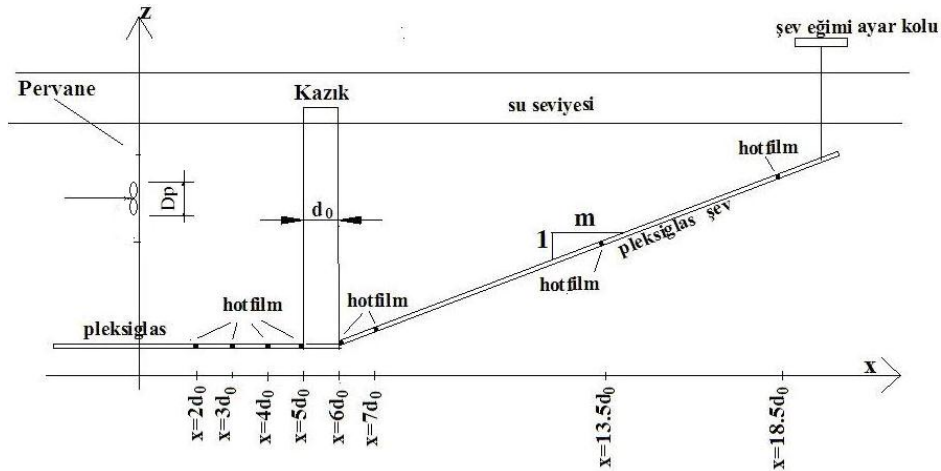


Figure 14 Experimental conditions for the open type wharf

The variation of the non-dimensional bed shear stress along the propeller jet axis for four different slopes are presented in Figure 17. The propeller jet velocities are varied with 560 rpm, 630 rpm and 695 rpm. The bed shear stress at different locations are non-dimensional respect to τ_0 which is the bed shear stress close the jet exit ($x=2d_0$).

The slopes were $s=0.0$, $1/1.5$, $1/2.0$ and $1/2.5$. Bed shear stress reaches maximum close the pile at the upstream but decreased at the downstream side of the pile. The shear stress slightly increase with increasing propeller jet velocity at the upstream of the pile.

The non-dimensional bed shear stresses along the propeller axis increase with increasing slope angle in Figure 18. The shear stresses at the downstream of the pile jump and they reach its maximum value for the steepest slope ($s=1/1.5$). The location where the shear stress has their maximum value present the impinging point of the propeller jet on the slope. It appears clearly for the steepest slope. The bed shear stress are jumped at the position $x=13.5d_0$ for the the slope of $1/1.5$.

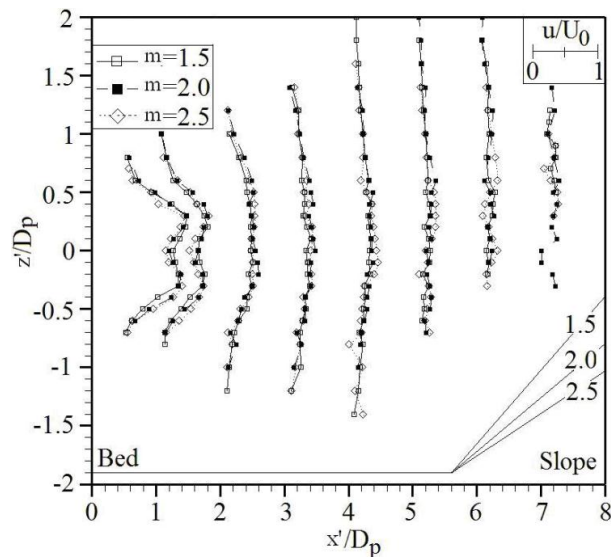


Figure 15 Propeller jet velocity profiles for different slopes.

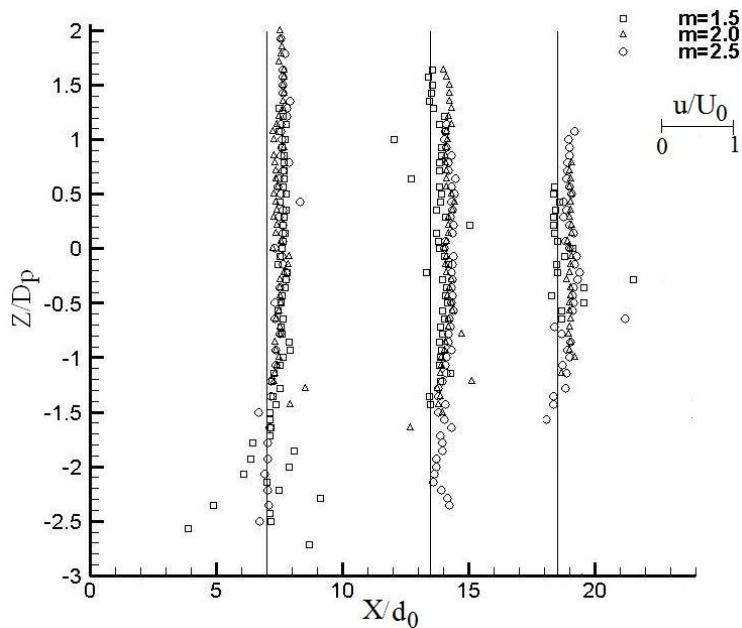


Figure 16 Propeller jet velocity profiles at the downstream of the pile the slopes for 40 Hz (Re=43290).

iii) Comparisons

When the velocity profiles of submerged wall jet and propeller jet are compared each other along x axis, the decrease of the velocity profiles for the propeller jet are faster than in case of the wall jet. But the velocity profile results for the propeller and wall jet behind the pile are similar. The bed shear stresses for both mechanisms increase in front of the pile. The decrease of the shear stress behind the pile for the propeller jet is faster than the wall jet case.

CONCLUSIONS

As flow Reynolds number increases, velocity and bed shear stresses increase for both wall jet and propeller jet. But the decrease is faster for the conventional propeller jet.

Measurements show that vertical velocities along the jet axis increase away from the pile at upstream of the pile, decrease away from the pile at downstream of the pile for the wall jet.

Bed shear stresses increase towards the pile along the jet axis at upstream and slowly decrease at the downstream of the pile. Maximum bed shear stress value is obtained at $\theta=75$ degree around the pile.

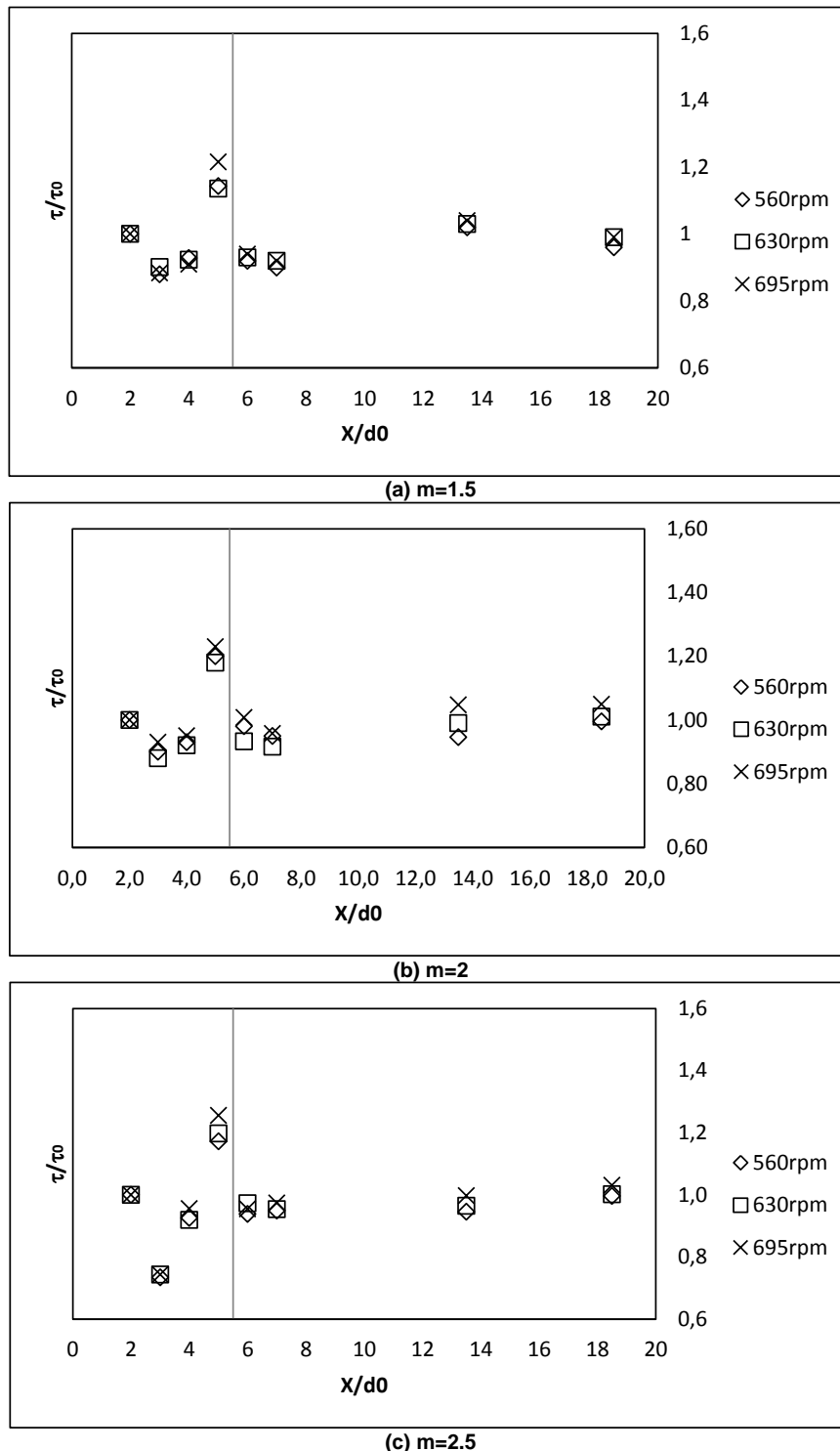


Figure 17 The variation of the bed shear stress along the jet axis with different jet velocities and slopes.

Bed shear stress for the propeller jet increase towards the pile and the decrease is faster behind the pile. But the shear stresses suddenly increase at the impinging point on the slope behind the pile. Erosion process over slopes occurred with increasing bed shear stress at the impinging point.

Shear stresses over the slopes decrease with decreasing of the slope angles. Maximum shear stresses on the slopes are measured at $x=13.5d_0$ for $s_1=1/1.5$ while $x=18.5d_0$ for $s_2=1/2$ and $s_3=1/2.5$. These causes more erosion for the steep slopes.

Propeller jet shows more decays than the free water jet case due to diffusion of the propeller jet. Bed shear stress variations and velocity profiles show similar tendency for both water jet and propeller jet.

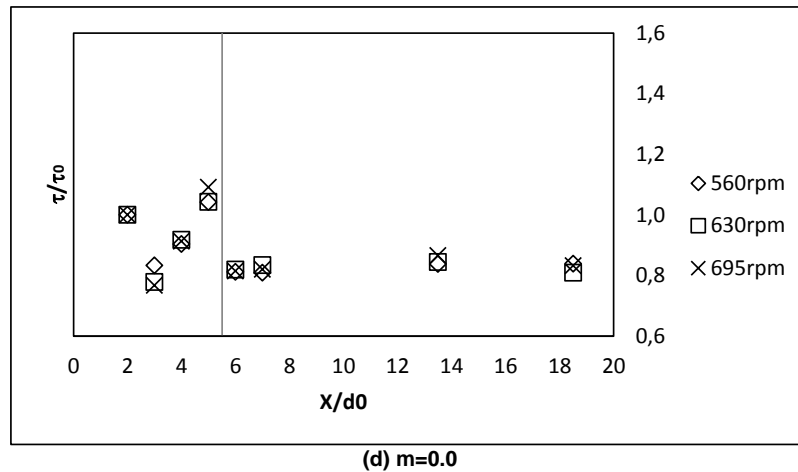


Figure 17 Continue

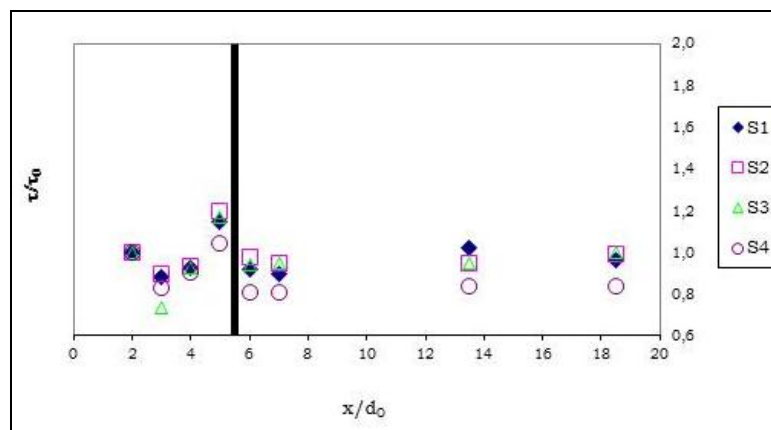


Figure 18 The variation of the bed shear stress along the jet axis with different slopes

REFERENCES

- Bergh, H., and Cederwall, K., 1981, Propeller erosion in harbours, *Bulletin No TRITA-VBI-107 Hydraulics Laboratory*, Royal Institute of Technology, Stockholm, Sweden.
- Billiton, BHP, 2010, *Assessment of Waves and Propeller Wash Associated with Shipping: Final Report*, AMOG Consulting, Australia.
- Blaauw, H. G., and Kaa, E. J. Van de (1978), *Erosion of bottom and sloping banks caused by the screw race of the maneuvering ships*, Publ. No. 202, Delft Hydraulics Laboratory, Delft, The Netherlands.
- Celikoglu, Y., Cihan, K., Sahin, E., Yüksel, Y., 2012, Propeller Jet Flow Around a Pile Type Structure, *COPEDEC 2012, PIANC*, Chennai, India.
- Cihan, K., Yüksel, A. and Yüksel, Y., 2012, The Effect of Slope Angle on the Propeller Jet Erosion near Quay Structures, *Maritime Engineering J., ICE*.
- Lam, W., Hamil, G.A., Song, Y.C., Robinson, D.J. and Raghunathan, S., 2011, A Review of the Equations Used to Predict the Velocity Distribution within a Ship's Propeller Jet, *J. of Ocean Engineering*, Vol.38, pp. 1-10.
- PIANC, 1997, *Guidelines for the Design of Armoured Slopes under Open Piled Quay Walls*, Bulletin 96, Brussels Belgium.
- Sumer, B.M. and Fredsoe, J., 2002, *The Mechanics of Scour in the Marine Environment*, Advanced Series Ocean Engineering, Vol.17, World Scientific.
- Schokking, L.A., 2002, *Bowthruster-induced Damage*, M.Sc. Thesis, Delft University of Technology.

- Verhey, H.J., 1983, The Stability of Bottom and Banks Subjected to the Velocities in the Propeller Jet Behind Ships, *Publication No:303, 8th International Harbour Congress*, Antwerp, Belgium, June 13-17.
- Veldhoven, V., van, 2001, *Vooronderzoek schroefstraal op een talud met breuksteen*, DUT M.Sc. Thesis.
- Yüksel, A. and Yüksel, A., 2010, Simulation of a 3D submerged jet flow around a pile, *Ocean Engineering*, Vol. 37, pp. 819-832.
- Whitehouse, R., 1998, *Scour at Marine Structures*, HR Wallingford, Thomas Telford.